Publications of the Astronomical Society of Australia (2018), **35**, e046, 9 pages
doi:10.1017/pasa.2018.33

CAMBRIDGE
UNIVERSITY PRESS

Research Paper

Calculation of molecular line intensity in stellar atmospheres

B. Barbuy, J. Trevisan and A. de Almeida
Universidade de São Paulo, IAG, Rua do Matão 1226, Cidade Universitária, São Paulo 05508-090, Brazil

Abstract

Molecular line intensity calculations are not a straightforward task. We present a description of the basics for including molecular lines in synthetic spectra and of the input data needed. We aim both at describing ways in which molecular lines are computed in the context of photospheres of F–G–K stars, and to present a new online available version of our code for spectrum synthesis of cool stars. We apply calculations to molecular bands in the ultraviolet, visible, and near-infrared main features, and comparisons with spectra of reference stars are shown. We provide user-friendly tools for the free use of the code PFANT. The code is available at http://trevisanj.github.io/PFANT.

Keywords: atmospheres – molecular lines – stars: abundances

(Received 08 March 2018; revised 26 June 2018; accepted 7 September 2018)

1. Introduction

Molecular bands in the spectra of cool stars need to be considered in the calculation of synthetic spectra of cool stars, first of all because they are present all over the spectra, affecting considerably the continuum, and because there are several strong lines. Bands involving C, N, O, in particular, are key indicators of many important aspects of both stellar evolution and chemical evolution. For example, photometric filters placed to measure CH, NH, CN, OH, as used in Piotto et al. (2015), can reveal multiple stellar populations in globular clusters.

The main nitrogen indicators used in the literature are CN bands, among which the strongest ones are in the near-UV, in particular CN(0,0) at 388.3 nm. For the use of CN, one has to previously derive C, available in the optical from the CH G-bandhead at 431 nm or a weak C_2(0,0) bandhead at 563.5 nm. In the near-UV, there is the unique available strong NH bandhead at 336 nm. The NH band measurement in important samples would allow a direct measurement of nitrogen (e.g. Pasquini et al. 2008). Note on the other hand that discrepancies have been found in the nitrogen abundances derived from CN and NH bandheads, still unsolved (see Spite et al. 2005).

Oxygen has several strong OH lines occurring in the near-UV, at $\lambda \lesssim 330$ nm, and in the near-infrared (NIR) in the H band. In metal-poor turn-off dwarf stars, the UV OH lines are the only measurable oxygen indicator. Furthermore, molecular bands of CH and CN in the visible and NIR are the best way of deriving the isotopic composition of, in particular, 12C/13C (e.g. Smith, Terndrup, & Suntzeff 2002), which is an indicator of stellar mixing (e.g. Smiljanic et al. 2009).

Therefore, the inclusion of molecular lines in synthetic spectra calculations of stars cooler than $\lesssim$7 000 K is of utmost importance. Line lists of molecular bands come however in different formats, and as well the different codes use these lists adapted in different ways. The main difference in using molecular line lists is the use of either the Einstein *A* coefficients, such as given in Goorvitch (1994) for the NIR lines of CO $X^1\Sigma^+$ system, which are a sum of all ingredients, or when this is not available, the different constituents that produce the line. In the present paper we aim to show how to use these different data.

Codes for spectrum synthesis available include about a dozen of them, among which SYNTHE (Kurúcz 1970, 1993a), MOOG (Sneden 1973), the codes BSYN (Edvardsson et al. 1993), and TURBOSPECTRUM (Alvarez & Plez 1998), from the Uppsala group, and SME (Valenti & Piskunov 1996; Piskunov & Valenti 2017), among a few others. In the present paper, we give details on the updated version of the spectrum synthesis code PFANT, which is now available online.

In Section 2 we describe the calculation of molecular lines of diatomic molecules. In Section 3 we describe the spectrum synthesis code PFANT and the line lists used. In Section 4 a short summary is given.

2. Molecular absorption coefficient

In the 1960s and early 1970s a few authors provided the basis for the understanding and correct calculation of molecular line formation. There are some inconsistencies in normalisation matters among these papers, which made the subject a hot topic at that time. These include Schadee (1964, 1967, 1975, 1978), Tatum (1967), and Whiting & Nicholls (1974). A particularly clear work on normalisation factors was given later by all these authors gathered in Whiting et al. (1980). In the following, a description on the calculation of diatomic molecular lines is given, trying to be as straightforward as possible, and in the next section these equations are included in the code PFANT presented in this paper.

The opacity of a molecular line as a result of a transition between two rotational levels is given by

Author for correspondence: B. Barbuy, Email: b.barbuy@iag.usp.br
Cite this article: Barbuy B, Trevisan J. and de Almeida A. Calculation of molecular line intensity in stellar atmospheres. *Publications of the Astronomical Society of Australia* **35**, e046, 1–9. https://doi.org/10.1017/pasa.2018.33

© Astronomical Society of Australia 2018; published by Cambridge University Press.

https://doi.org/10.1017/pasa.2018.33 Published online by Cambridge University Press

$$\kappa_{\rm mol} = \frac{\pi e^2}{m_{\rm e} c^2} \lambda^2_{0J'J''} f N''_{nvj} \frac{H(a,\nu)}{\sqrt{\pi}\,\Delta\lambda_{\rm D}} \left(1 - e^{\frac{-hc}{\lambda_{0J'J''}kT}}\right), \quad (1)$$

where f is the molecular oscillator strength, $\lambda^2_{0J'J''}$ is the line central wavelength, J is the rotational quantum number, v is the vibrational quantum number, n is the electronic quantum number, N''_{nvj} is the population of the lower level, and $\Delta\lambda_{\rm D}$ is the Doppler width given by

$$\Delta\lambda_{\rm D} = \frac{\lambda_0}{c}\sqrt{\frac{2kT}{M} + v_t^2}, \quad (2)$$

where v_t is the microturbulence velocity, c is the light speed (2.997×10^8 m/s), $m_{\rm e}$ is the mass of hydrogen (1.6737236×10^{-24} g), and e is the electron charge (1.6022×10^{-19} C). Finally, $H(a,v)$ is the Hjerting's function for line wing broadening, where $v = \frac{\Delta\lambda}{\Delta\lambda_{\rm D}}$; the damping constant $\Gamma = \lambda^2/4\pi c\Delta\lambda_{\rm D}$, where a is the damping parameter (see, e.g. Gray 2005).

2.1. Line strength and Einstein coefficients

Einstein (1917) introduced the A and B coefficients to describe spontaneous emission, and induced absorption and emission. The Einstein A coefficient is defined in terms of spontaneous emission from level 2 to level 1 by the probability: $\mathrm{d}W = A_{21}\mathrm{d}t$. In a radiation field with a radiation density ρ_ν at frequency ν, a transition from 1 to 2 has probability $\mathrm{d}W = B_{12}\rho_\nu \mathrm{d}t$, and also induced emission with the probability $\mathrm{d}W = B_{21}\rho\mathrm{d}t$. In a system with N_1, N_2 atoms in levels 1 and 2, the total rate of transitions is $W_{21} = A_{21}N_2$ for spontaneous emission, $W_{12} = B^\nu_{12}\rho_\nu N_1$ for induced absorption, and $W_{21} = B^\nu_{21}\rho_\nu N_2$ for induced emission. He also showed that $B^\nu_{21} = (\pi^2c^3/h\nu^3_{21})A_{21}$ and $B^\nu_{12} = (g_2/g_1)B^\nu_{21}$, where g is the degeneracy factor.

The line intensity resulting from a spontaneous photon emission in a rotational transition from levels (J', J'') is

$$E_{J'J''} = N_{J'} h\nu_{J'J''} A_{J'J''}, \quad (3)$$

where J', J'' are the rotational quantum numbers of upper and lower levels of the transition, respectively.

The Einstein probability coefficient for a rotational transition $J'J''$ between two levels $(n'v'\Lambda'J'p', n''v''\Lambda''J''p'')$ will be

$$A_{J'J''} = \frac{64\pi^4\nu^3}{3hc^3 d}\sum_{M'M''} |\mathbf{R}_{n'v'\Lambda'J'p',n''v''\Lambda''J''p''}|^2 = \frac{64\pi^4\nu^3}{3hc^3 d}\mathcal{S}, \quad (4)$$

where $\mathcal{S}$ is the line strength, Λ is the electronic sublevel of spin, p is the parity (due to dedoubling of rotational states), M is the magnetic quantum number, d is the degeneracy; R_{ij} are the elements of the matrix of electric dipole moment = transition moments, and $|\mathbf{R}|^2$ is the transition probability. Note that each rotational level J has $(2J+1)$ sublevels characterised by a quantum number M. Each of the two states of Λ doubling is considered a distinct rotational state (according to Whiting & Nicholls 1974 and contrariwise to Tatum 1967 and Schadee 1971).

2.2. Transition moments R

The transition moment R is defined as

$$R_{ij} = \int_{-\infty}^{\infty} \Psi_i^* P \Psi_j \mathrm{d}V \quad (5)$$

or, in Dirac's notation,

$$R_{ij} = \langle \Psi_i \mid \mathbf{P} \mid \Psi_j \rangle, \quad (6)$$

corresponding to transition moments for a transition between two states (i, j) such as (J', J'') or (v', v'') etc., where Ψ_i, Ψ_j are total wave functions of states i and j, and $\mathbf{P}$ is the electric dipole moment.

Hönl & London (1925) have shown that the wave function can be separated in radial and angular parts, such that the transition moment can be written as

$$\sum_{M'M''} |\mathbf{R}^{n'v'\Lambda'p'J'}_{n''v''\Lambda''p''J''}|^2 = \sum_{M'M''} |\mathbf{R}_{nv\Lambda pJ}|^2 = \mathcal{S}_{nv\Lambda pJ} = R^{\rm nv}_{\rm rad}\mathscr{S}_{\Lambda pJ}. \quad (7)$$

The superscript 'nv' symbolises the dependence of $R^{\rm nv}_{\rm rad}$ on the electronic and vibrational eigenfunctions.

2.2.1. The vibronic transition moment $R^{\rm nv}_{\rm rad}$

The Born–Oppenheimer approximation (1927) allows the wave function of a molecule to be broken into two components, the electronic and the nuclear (vibrational and rotational), given that the electronic wave function varies very slowly with the nuclear coordinates. Therefore,

$$\Psi_{\rm total} = \Psi_{\rm electronic} \times \Psi_{\rm nuclear}. \quad (8)$$

The dipole moment can thus be broken into two components, electronic and nuclear, that is, $\mathbf{P} = \mathbf{P}_{\rm e} + \mathbf{P}_{\rm N}$. The transition moment becomes then

$$\mathbf{R}_{\rm rad} = \int_{-\infty}^{\infty} \Psi_{\rm e}^{'*}\Psi_{\rm v}^{'*}(\mathbf{P}_{\rm e} + \mathbf{P}_{\rm N})\Psi_{\rm e}^{''}\Psi_{\rm v}^{''}\mathrm{d}V, \quad (9)$$

and $\mathrm{d}V$ is defined by electronic and nuclear coordinates: $\mathrm{d}V = \mathrm{d}V_{\rm e}\mathrm{d}V_{\rm N}$ or, since $\Psi_{\rm v}$ and $\mathrm{P}_{\rm N}$ are functions only of the internuclear distance r, the formula can be reduced to a radial dependence only; therefore,

$$\mathbf{R}_{\rm rad} = \int_{-\infty}^{\infty} \Psi_{\rm v}^{'*}(\Psi_{\rm e}^{'*}\mathbf{P}_{\rm e}\Psi_{\rm e}^{''}\mathrm{d}V_{\rm e})\Psi_{\rm v}^{''}\mathrm{d}r + \int_{-\infty}^{\infty} \Psi_{\rm v}^{'*}\mathbf{P}_{\rm N}(\Psi_{\rm e}^{'*}\Psi_{\rm e}^{''*}\mathrm{d}V_{\rm e})\Psi_{\rm v}^{''}\mathrm{d}r. \quad (10)$$

The wave functions of different electronic states are orthogonal; therefore, the second term of this equation can be cancelled. The electronic transition moment can be defined as

$$\mathbf{R}_{\rm e} = \int_{-\infty}^{\infty} \Psi_{\rm e}^{'*}\mathbf{P}_{\rm e}\Psi_{\rm e}^{''}\mathrm{d}V_{\rm e} = < \Psi_{\rm e}^{'*} \mid \mathbf{P}_{\rm e} \mid \Psi_{\rm e}^{''} >, \quad (11)$$

$$\mathbf{R}_{\rm rad} = \int_{-\infty}^{\infty} \Psi_{\rm v}^{'*}\mathbf{R}_{\rm e}\Psi_{\rm v}^{''}\mathrm{d}r, \quad (12)$$

where $\mathbf{R}_{\rm e}$ can be measured in laboratory experiments, or computed theoretically. As a first approximation, we can admit that $\mathbf{R}_{\rm e}$ = constant, and a mean value can be adopted:

$$\mathbf{R}_{\rm rad} = \mathbf{R}_{\rm e}\int_{-\infty}^{\infty} \Psi_{\rm v}^{'*}\Psi_{\rm v}^{''}\mathrm{d}r, \quad (13)$$

where the Franck–Condon factor is

$$q_{v'v''} = \left|\int_{-\infty}^{\infty} \Psi_{\rm v}^{'*}\Psi_{\rm v}^{''}\mathrm{d}r\right|^2, \quad (14)$$

and the band intensity (*force de bande*) is

$$R^{\rm nv}_{\rm rad} = R^{\rm ev}_{\rm rad} = |\mathbf{R}_{\rm e}|^2 q_{v'v''}. \quad (15)$$

2.2.2. The line strength $\mathcal{S}$

The line strength for rotational lines will be (Whiting et al. 1980)

$$\mathcal{S} = |\mathbf{R}_{\rm e}|^2 q_{v'v''}\mathscr{S}_{J'J''}, \quad (16)$$

https://doi.org/10.1017/pasa.2018.33 Published online by Cambridge University Press

with $\mathscr{S}_{J'J''} = \mathscr{S}_{\Lambda pJ}$ = Hönl–London factor (HLF), giving the relative intensity of the different rotational transitions. Depending on the Hund's coupling associated with each case, formulae for computing the HLF are tabulated by Kovács (1969).

The normalisation of the HLF is as follows, valid for all cases of Λ–S coupling (Whiting et al. 1980):

$$\sum \mathscr{S}_{J'J''}(J) = (2 - \delta_{0,\Lambda'+\Lambda''})(2S+1)(2J+1), \tag{17}$$

where the sum is carried out for all branches and fixed J. The Kronecker delta $\delta_{0,\Lambda'+\Lambda''}$ equals 1 for $\Sigma-\Sigma$ transitions and 0 otherwise. The term $(2 - \delta_{0,\Lambda'+\Lambda''})(2S+1)$ represents the degeneracy of the electronic state, $(2J+1)$ the degeneracy of each rotational level, and $(2S+1)$ represents the multiplicity of the transition: 1 for singlet, 2 for doublet, etc.

2.2.3. The oscillator strength f

The oscillator strength f is defined as

$$f = f_{J'J''} = f^{n'v'\Lambda'p'J'}_{n''v''\Lambda''p''J''} = f_{nv\Lambda pJ} = \frac{8\pi^2 m_e \nu}{3he^2 d} \sum_{M'M''} |\mathbf{R}_{n'v'\lambda'J'p',n''v''\lambda''J''p''}|^2 \tag{18}$$

$$= \frac{8\pi^2 m_e \nu_{J'J''}}{3he^2 d} |\mathbf{R}_e|^2 q_{v'v''} \mathscr{S}_{J'J''} = \frac{8\pi^2 m_e \nu}{3he^2 d} \mathcal{S}.$$

Therefore, by combining Equations (4) and (18), we get

$$\frac{A}{f} = \frac{8\pi^2 \nu^2 e^2}{c^3 m_e}. \tag{19}$$

Designating $f_{v'v''}$ as vibronic oscillator strength, we have

$$f_{v'v''} = \frac{8\pi^2 m_e \nu}{3he^2} R^{\mathrm{nv}}_{\mathrm{rad}} = \frac{8\pi^2 m_e \nu_{J'J''}}{3he^2} |\mathbf{R}_e|^2 q_{v'v''}; \tag{20}$$

therefore,

$$f = \frac{f_{v'v''} \mathscr{S}_{J'J''}}{d}. \tag{21}$$

The degeneracy factor d is $(2J''+1)$ for a single rotational line:

$$f^{n'v'\Sigma'p'J'}_{n''v''\Sigma''p''J''} = \frac{f_{v'v''} \mathscr{S}_{J'J''}}{(2J''+1)}. \tag{22}$$

The molecular absorption coefficient can then be expressed by

$$\kappa\mathrm{mol} = \frac{\pi e^2}{m_e c^2} \lambda^2_{0J'J''} f_{v'v''} \frac{\mathscr{S}_{\Lambda pJ}}{(2J''+1)} N''_{nvj} \times \frac{H(a,v)}{\sqrt{\pi}\,\Delta\lambda_D} \left(1 - e^{\frac{-hc}{\lambda_{0J'J''}kT}}\right), \tag{23}$$

2.3. Calculation of the lower level population N''_{nvj}

Consider the equilibrium reaction A + B ⇌ AB, between two atoms A and B, of the AB molecule, which is expressed by the relation:

$$\frac{n(\mathrm{A})n(\mathrm{B})}{n(\mathrm{A})} = \frac{\left(\sum_i g_i e^{-\epsilon_i/kT}\right)_{\mathrm{A}} \left(\sum_i g_i e^{-\epsilon_i/kT}\right)_{\mathrm{B}}}{\left(\sum_i g_i e^{-\epsilon_i/kT}\right)_{\mathrm{AB}}} = \frac{Q_{\mathrm{total_A}} Q_{\mathrm{total_B}}}{Q_{\mathrm{total_{AB}}}}, \tag{24}$$

where g_i is the statistical weight, $n(X)$ is the number of particles X in a volume $V(X)$, $Q_{\mathrm{total}} = Q_{\mathrm{translational}} Q_{\mathrm{internal}} = \left(\sum_i g_i e^{-\epsilon_i/kT}\right)$ = total partition function, and the energies $(\epsilon_i)_{\mathrm{A}}$, $(\epsilon_i)_{\mathrm{B}}$ are defined with respect to the fundamental state, that is, $(\epsilon_i)_{\mathrm{A,B}} = [(\epsilon_0)_{\mathrm{fundamentalstate}} + (\epsilon_i)_{\mathrm{exc}}]_{\mathrm{A,B}}$. The AB molecule energies $\epsilon_i/kT_{\mathrm{AB}}$ are given relative to the vibrational fundamental state (quantum number $v=0$), of the fundamental electronic state of the molecule: $(\epsilon_i)_{\mathrm{AB}} = [(\epsilon_0)_{\mathrm{fundamentalstate}}(v=0) + (\epsilon_i)_{\mathrm{exc}}]_{\mathrm{AB}}$.

By rewriting Equation (24), we have

$$\frac{n(\mathrm{A})n(\mathrm{B})}{n(\mathrm{A})} = \frac{Q_{\mathrm{A}} Q_{\mathrm{B}}}{Q_{\mathrm{AB}}} e^{-(\epsilon_{0_{\mathrm{A}}} + \epsilon_{0_{\mathrm{B}}} - \epsilon_{0_{\mathrm{AB}}})/kT}, \tag{25}$$

where $\epsilon_{0_{\mathrm{A}}} + \epsilon_{0_{\mathrm{B}}} - \epsilon_{0_{\mathrm{AB}}} = D_0$, and D_0 is the dissociation energy of molecule AB.

Noting that $Q_{\mathrm{translational}} = \left(\frac{2\pi mkT}{h^2}\right)^{3/2} V$, we get

$$\frac{n(\mathrm{A})n(\mathrm{B})}{n(\mathrm{A})} = \left(\frac{2\pi mkT}{h^2}\right)^{3/2} \frac{V_A V_B}{V_{\mathrm{AB}}} \mu^{3/2}_{\mathrm{AB}} \times \frac{Q_{\mathrm{int_A}} \times Q_{\mathrm{int_B}}}{Q_{\mathrm{int_{AB}}}} e^{-D_0/kT}, \tag{26}$$

where $\mu_{\mathrm{AB}} = m_{\mathrm{A}} m_{\mathrm{B}}/m_{\mathrm{AB}}$ is the reduced mass.

On the other hand, the definition of the dissociation pressure constant is

$$K^P_{\mathrm{AB}} = \frac{p_{\mathrm{A}}\, p_{\mathrm{B}}}{p_{\mathrm{AB}}}, \tag{27}$$

where p_{A}, p_{B}, and p_{AB} are the partial pressures of particles A, B, and AB.

$$\frac{p_{\mathrm{A}}\, p_{\mathrm{B}}}{p_{\mathrm{AB}}} = \left(\frac{2\pi kT}{h^2} \mu_{\mathrm{AB}}\right)^{3/2} \frac{Q_{\mathrm{int_A}}\, Q_{\mathrm{int_B}}}{Q_{\mathrm{int_{AB}}}} kT\, e^{\frac{-D_0}{kT}}. \tag{28}$$

Considering now the Boltzmann equation for the population of the level nvJ, $(N_{\mathrm{AB}})_{nvJ}$ being the number of molecules AB in the electronic level n, vibrational level v, and rotational level J, per volume unit, and N_{AB} the total number of molecules AB per volume unit, we have

$$\frac{(N_{\mathrm{AB}})_{nvJ}}{N_{\mathrm{AB}}} = \frac{(Q_{\mathrm{int_{AB}}})_{nvJ}}{Q_{\mathrm{int_{AB}}}}, \tag{29}$$

and one obtains

$$\frac{(N_{\mathrm{AB}})_{nvJ}}{N_{\mathrm{AB}}} = \left(\frac{2\pi kT}{h^2} \mu_{\mathrm{AB}}\right)^{-3/2} \frac{N_{\mathrm{A}} N_{\mathrm{B}}}{Q_{\mathrm{int_A}}\, Q_{\mathrm{int_B}}} Q_{\mathrm{int_{AB}}}\, e^{\frac{D_0}{kT}}. \tag{30}$$

2.4. The partition functions $Q_{\mathrm{int_{AB}}}$

Considering that for a molecule, the electronic, vibrational, and rotational energies are independent of each other, Q_{int} may be written as the product:

$$Q_{\mathrm{int}} = Q_{\mathrm{el}}\, Q_{\mathrm{vibr}}\, Q_{\mathrm{rot}}, \tag{31}$$

where

$$Q_{\mathrm{el}} = g_{\mathrm{el}}\, e^{\frac{-T_e hc}{kT}}, \tag{32}$$

$$Q_{\mathrm{vibr}} = g_{\mathrm{vibr}}\, e^{\frac{-G(v)hc}{kT}}, \tag{33}$$

$$Q_{\mathrm{rot}} = g_{\mathrm{rot}}\, e^{\frac{-F(J)hc}{kT}}, \tag{34}$$

and

(a) g_{el}, g_{vibr}, and g_{rot} are the statistical weights of the electronic, vibrational, and rotational levels, respectively. The product of the statistical weight g_{el}, g_{vibr}, and g_{rot} is given for each case of molecular transition by Tatum (1967);

(b) T_e is the term value of electronic energy of a multiplet, in first approximation it is given by

$$T_e = T_0 + A\Lambda\Sigma, \tag{35}$$

where T_0 is the value of the term if the spin is negligible, A is the constant of spin coupling; Λ and Σ are, respectively, orbital electronic angular momentum and spin angular momentum, projected in the internuclear axis (not to confound with other A and Λ defined in Section 2.1).

https://doi.org/10.1017/pasa.2018.33 Published online by Cambridge University Press

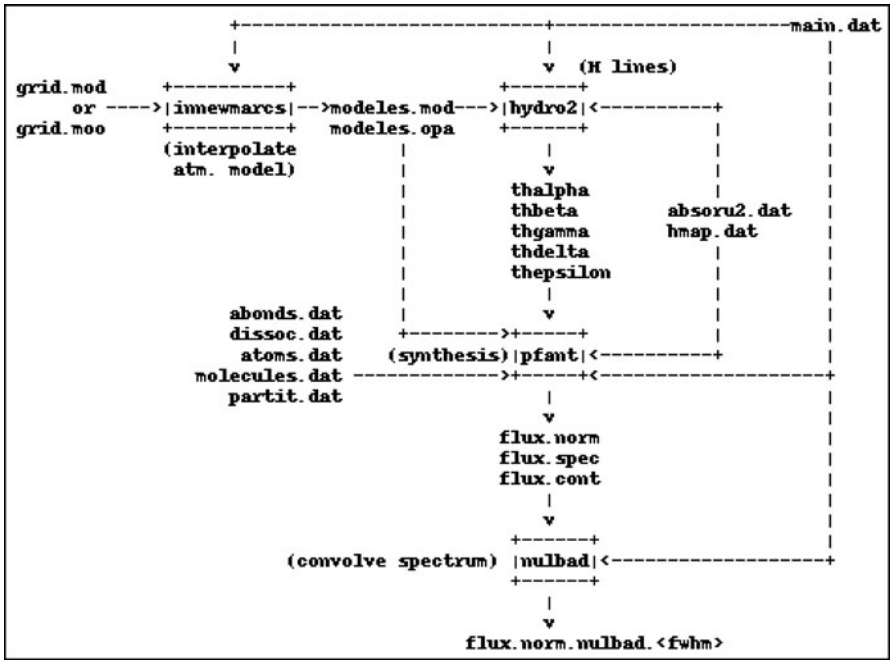

Figure 1. PFANT workflow. Boxes represent the FORTRAN binaries; unboxed text represent input/output files. *Source*: PFANT manual.

(c) $F(J)$ is the term of rotational energy, given by

$$F(J) = B_v J(J+1) - D_v J^2 (J+1)^2 \ldots, \tag{36}$$

where B_v is the rotational constant and D_v is the centrifugal distortion constant.

Note: $F(J)$ is given with respect to the lowest level, that is, $F(J)$ is in reality $F(J) - F(1)$.

(d) $G(v)$ is the term of vibrational energy.

A diatomic molecule, by the vibrational movements of its nuclei, can be treated as an anharmonic oscillator with a potential U approximately given by

$$U = f(r - r_e)^2 - g(r - r_e)^3, \tag{37}$$

where: $g \ll f$ and r_e is the internuclear distance in equilibrium.

Introducing U in the wave equation, one obtains the following energy eigenvalues:

$$E_v = hc \left\{ \omega_e \left(v + \frac{1}{2}\right) - \omega_e x_e \left(v + \frac{1}{2}\right)^2 + \omega_e y_e \left(v + \frac{1}{2}\right)^3 + \ldots \right\}$$
$$= hc\, G(v) \tag{38}$$

The values of the anharmonic constants ω_e, $\omega_e x_e$, and $\omega_e y_e$ are tabulated in the literature (for example, in Huber & Herzberg 1979, or in the NIST Chemistry web book at http://webbook.nist.gov/chemistry).

Note: $G(v)$ is given with respect to the zero point energy, that is, $v = 0$, so in reality one uses $G_0(v) = G(v) - G(0)$.

A discussion on the multiple forms used for partition functions is presented in Popovas (2014).

3. PFANT: calculation of synthetic spectra

The spectra were computed using the code PFANT[a]. The first version of this FORTRAN code, named FANTOM, was developed by Spite (1967) for the calculation of atomic lines. Barbuy (1982) included the calculation of molecular lines, implementing the dissociative equilibrium by Tsuji (1973) and molecular line computations as described in Cayrel et al. (1991). It has been further improved for calculations of large wavelength coverage and inclusion of hydrogen lines as described in Barbuy et al. (2003), where M. N. Perrin had an important rôle, wherefrom comes the P in PFANT. Coelho et al. (2005) unified the code to contain the full line lists from the ultraviolet (Castilho et al. 1999), together with the visible (Barbuy et al. 2003), and near-infrared (Meléndez et al. 2001).

Given a stellar model atmosphere and lists of atomic and molecular lines, the code computes a synthetic spectrum assuming local thermodynamic equilibrium (LTE).

[a]http://trevisanj.github.io/PFANT

3.1. New changes to the PFANT code

During 2015–2017, the code was entirely upgraded with homogenisation of language to FORTRAN 2003, optimisation for speed, improved error reporting in case of problems with the input data files, and command-line configuration options. The code now has a manual including installation and tutorial sections.

Important existing accessory codes in FORTRAN were also upgraded and incorporated to form a four-step workflow as follows (Figure 1):

1. `innewmarcs`—interpolate a grid of MARCS atmospheric models (Gustafsson et al. 2008) to generate star-specific model (the original code comes from the Meudon research group);
2. `hydro2`—calculate hydrogen lines profiles (Praderie 1967);
3. `pfant`—calculate synthetic spectrum;
4. `nulbad`—convolve synthetic spectrum with a Gaussian profile to simulate spectral measurement.

The list above describes commands to be typed in a computer terminal. All commands may be invoked with the `--help` option.

https://doi.org/10.1017/pasa.2018.33 Published online by Cambridge University Press

3.2. Input and output data

This section describes the most relevant data files needed or generated during PFANT code execution. The following subsections refer to these files by their default names, which can be changed via command line if necessary.

3.2.1. Stellar parameters and abundances

Stellar parameters and chemical abundances are defined in files `main.dat` and `abonds.dat`. The code available for download includes reference solar abundances that can be chosen to be those from Asplund et al. (2009), Grevesse et al. (1996), Scott et al. (2015a, 2015b) and Grevesse et al. (2015), or Grevesse et al. plus $A(O)$=8.76 from Steffen et al. (2015).

3.2.2. Model atmospheres

`innewmarcs`, the grid interpolation code, allows to call for a chosen grid among the MARCS model atmospheric grids (Gustafsson et al. 2008), and interpolates for the stellar parameters needed, creating files named `modeles.mod` and `modeles.opa`. If these parameters, that is, $\mathbf{v} = (T_{\rm eff}, \log g, [{\rm Fe/H}])$ are outside the grid, the code does not extrapolate, but either stops or if forced to run (`innewmarcs --allow T`), projects $\mathbf{v}$, onto closest grid 'wall', then interpolates.

It is possible to replace the grid among the different options given in MARCS. To create a new grid, it suffices to download the atmospheric models of interest (files '.mod' and '.opa') from the MARCS website (http://marcs.astro.uu.se), place them in a single folder, and run `create-grid.py` (a PYTHON script included with the `pyfant` package, described in Section 3.3).

3.2.3. Hydrogen lines profiles

The Balmer, Paschen, and Brackett series line data are included in file `hmap.dat`. For each hydrogen line, the central wavelength, the levels of the transition, excitation potential, and a constant related with the oscillator strength are tabulated. Hydrogen lines profiles are computed through a revised version of the code presented in Praderie (1967) (`hydro2`), generating separate files for each hydrogen line.

It is well known that hydrogen lines in red giant stars cannot be well reproduced. Cayrel et al. (1991) suggested that the bottom of the lines would be due to chromospheric layers, which are not taken into account in stellar atmosphere models. For higher order Balmer lines the overlapping of lines is taken into account, but combined with the Balmer decrement present in the continuum opacities, we get a bump in the continuum at 3 650–3 662 Å. This particular region should be used with caution.

3.2.4. Continuum opacity

The code `pfant` computes the continuum in pure absorption. It takes into account absorption due to H^-, H, H_2^+, He, and He^+, Rayleigh diffusion by H and H_2 and Thomson diffusion by electrons. A validation of these continuum calculations was carried out by Trevisan et al. (2011), through comparisons with the Uppsala code BSYN (Edvardsson et al. 1993, and updates since then). All steps of the calculation were carefully compared: optical depths of lines, continuum opacities κ_c, line broadening, and final abundances.

The inclusion of continuum from scattering is taken into account by adding the scattering opacity from the MARCS models. This is illustrated in Figure 2 for the stellar parameters

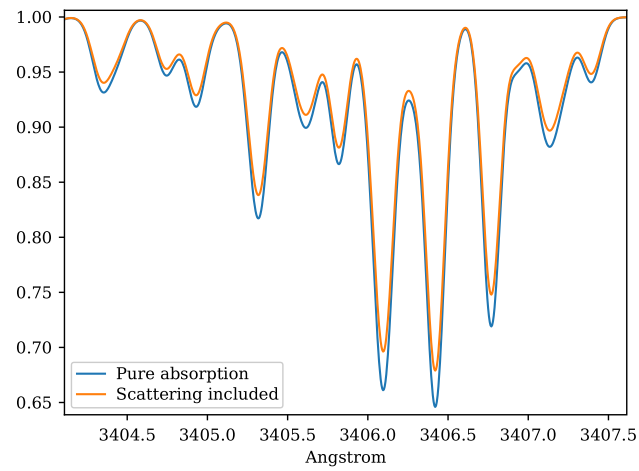

Figure 2. Synthetic spectra for star HP1-2115 with ($T_{\rm eff} = 4\,530$, $\log g = 2.0$, $[{\rm Fe/H}] = -1.0$, $v_{\rm t} = 1.45$), illustrating the change in the continuum, with both absorption and scattering (blue spectrum), and considering pure absorption (orange spectrum).

of star HP1-2115 with ($T_{\rm eff} = 4\,530$, $\log g = 2.0$, $[{\rm Fe/H}] = -1.0$, $v_{\rm t} = 1.45$) (Barbuy et al. 2016), in the near-ultraviolet, where this effect is more pronounced. MARCS opacities are interpolated by `innewmarcs` using a grid of atmospheric models with opacities included (`grid.moo`), generating file `modeles.opa`, which is identical in structure to '.opa' files downloaded from MARCS website. A similar calculation was presented in Figure 1 of Barbuy et al. (2011), based on calculations by B. Plez using the code TURBOSPECTRUM.

3.2.5. Atomic line lists

Atomic line lists can be converted from VALD3 (extended format) (Piskunov et al. 1995, Ryabchikova et al. 2015) lists of atomic lines. The VALD atomic line list started with basically the list by Kurúcz (1995, 2017), with progressive implementation of improvements coming from different sources. The default atomic line list in the range 3 000–10 000 Å is from VALD, where the collisional broadening is obtained by adopting a general formula for the van der Waals broadening (e.g. Gray 2005). Better broadening constant values can be obtained through the code from Anstee & O'Mara (1995), Barklem & O'Mara (1997), Barklem, Anstee, & O'Mara (1998), and Barklem, Piskunov, & O'Mara (2000) (this series of papers is referred to hereafter as ABO) for neutral lines.

The list of lines in the NIR adopted is from Meléndez & Barbuy (1999). An up-to-date such line list is given by Shetrone et al. (2015).

Other options of line lists are available, in particular, our own list that includes damping parameters from ABO for most lines in the visible region, and lists of hyperfine structure for several elements, that can be obtained by contacting the authors.

3.2.6. Molecular line lists

The list of molecules, their system, wavelength coverage, number of vibrational transitions (v', v''), the constants dissociation potential D_0 (eV), and the electronic oscillator strength $f_{\rm el}$, that is related to the transition moment $\mathbf{R}_e$, with corresponding references are given in Table 1. This list of molecular lines is included in the code package, in file `molecules.dat`.

In the near-ultraviolet and visible, the line lists from Kurúcz[b] were adopted (and transformed to our format) for OH and CN

[b] http://kurucz.harvard.edu/molecules.html

https://doi.org/10.1017/pasa.2018.33 Published online by Cambridge University Press

Table 1. Molecular lines included in PFANT and respective sources of data: line lists, dissociation potential $D_\circ$, electronic oscillator strength f_{el}

Molecule	System	No. lines	λλ(nm)	No. (v', v'')	Linelists	$D_\circ$(eV)	f_{el} (Ref.)
MgH	$A^2\Pi - X^2\Sigma$	1 945	470−609	13	(1)	1.34 (14)	0.2793 (17)
C_2 Swan	$d^3\Pi - a^3\Pi$	11 254	428−677	35	(2)	6.21 (15)	0.033 (18)
CN blue	$B^2\Sigma - X^2\Sigma$	92 851	300−600	197	(3)	7.72 (16)	0.0388 (19)
CN red	$A^2\Pi - X^2\Sigma$	23 828	483−2 715	88	(4)	"	0.00676 (20)
CH-AX	$A^2\Delta - X^2\Pi$	10 137+13 830[a]	321−787	20+31[a]	(5)	3.46 (14)	0.005257 (21)
CH-BX	$B^2\Sigma - X^2\Pi$	2 016	360−683	10	(5)	"	0.0025 (22)
CH-CX	$C^2\Sigma - X^2\Pi$	2 829	269−425	12	(5)	"	0.00595 (23)
CO-NIR	$X^1\Sigma^+$	7 088	1 557−5 701	63	(6)	11.09 (14)	– (24)
NH blue	$A^3\Pi - X^3\Sigma$	8 599	300−600	55	(7)	3.47 (14)	0.008 (22)
OH blue	$A^2\Sigma - X^2\Pi$	6 018	300−540	46	(3)	4.39 (14)	0.0008 (22)
OH-NIR	$X^2\Pi$	2 028	746−25 294	43	(8,9)	"	– (24)
FeH	$A^4\Delta - X^4\Delta$	2 705	778−1 634	9	(10)	1.63 (16)	0.001 (25)
TiO γ	$A^3\Phi - X^3\Delta$	26 007	622−879	23	(11,12,13)	6.87 (14)	0.15 (11)
TiO γ'	$B^3\Pi - X^3\Delta$	219 367	500−915	81	(11,12,13)	"	0.14 (11)
TiO α	$C^3\Delta - X^3\Delta$	360 726	388−837	79	(11,12,13)	"	0.12 (11)
TiO β	$c^1\Phi - a^1\Pi$	91 805	431−796	63	(11,12,13)	"	0.006 (11)
TiO δ	$b^1\Pi - a^1\Delta$	189 019	622−1 480	66	(11,12,13)	"	0.05 (11)
TiO ϵ	$E^3\Pi - X^3\Delta$	253 755	641−1 341	61	(11,12,13)	"	0.014 (11)
TiO ϕ	$b^1\Pi - d^1\Sigma$	105 082	664−1 800	65	(11,12,13)	"	0.052 (11)

References: (1) Balfour & Cartwright (1976); (2) Phillips & Davis (1968); (3) Kurúcz (1993*a*); (4) Davis & Phillips (1963); (5) Luque & Crosley (1999); (6) Goorvitch (1994); (7) Fernando et al. (2018); (8) Abrams et al. (1994); (9) Goldman et al. (1998); (10) Phillips et al. (1987); (11) Alvarez & Plez (1998); (12) Jorgensen (1994); (13) Plez (1998); (14) Huber & Herzberg (1979); (15) Pradhan, Partridge, & Bauschlicher (1994); (16) Schultz & Armentrout (1991); (17) Henneker & Popkie (1971); (18) Kirby, Saxon, & Liu (1979); (19) Duric, Erman, & Larsson (1978); (20) Bauschlicher, Langhoff, & Taylor (1988); (21) Brzozowski et al. (1976); (22) Grevesse & Sauval (1973); (23) Lambert (1978); (24) Goldman et al. (1998); (25) Schiavon et al. (1997).
[a] 12CH + 13CH.

blue. CH lines are from Luque & Crosley (1999). MgH lines are from Balfour & Cartwright (1976). The NH blue lines are adopted from the recent line lists by Fernando et al. (2018). The CN red and C_2 Swan lines are from C_2 laboratory line lists by Phillips & Davis (1968), and CN $A^2\Pi - X^2\Sigma$ red line lists by Davis & Phillips (1963). TiO line lists are from Alvarez & Plez (1998), Plez (1998), and Jorgensen (1994)—see Schiavon & Barbuy (1999). FeH line lists are from Phillips et al. (1987), and constants are described in Schiavon, Barbuy, & Singh (1997).

Note that the MgH, CN red, C_2, and FeH adopted correspond to laboratory measurements, differently to line lists available in most of the other codes.

In the NIR, the CO $X^1\Sigma$ lines are from Goorvitch (1994). The OH $X^2\Pi$ lines were made available by S. P. Davis that were originally from Abrams et al. (1994) with a few theoretical lines from Goldman et al. (1998)—see Meléndez & Barbuy (1999) and Meléndez, Barbuy, & Spite (2001).

Next we describe the structure of the PFANT molecular line lists files, which are hierarchically organised as follows:

1. for each molecular system: constants including the electronic oscillator strength f_{el} and dissociation constant D_0
2. for each (v', v'') transition in each molecular system: $q_{v'v''}$, $G_0(v)$, B_v, D_v
3. for each molecular line in each (v', v'') transition: $\lambda_{0J'J''}$, J'', $(\mathscr{S}_{\rm norm})_{J'J''}$, where (using Equation (17))

$$(\mathscr{S}_{\rm norm})_{J'J''} = \frac{\mathscr{S}_{J'J''}}{(2-\delta_{0,\Lambda'+\Lambda''})(2S+1)(2J+1)}, \tag{39}$$

so that (sum for all branches, fixed J)

$$\sum (\mathscr{S}_{\rm norm})_{J'J''} = 1. \tag{40}$$

$G_0(v)$, B_v, D_v are calculated as follows:

$$B_v = B_e - \alpha_e(v+0.5),$$
$$D_v = (D_e + \beta_e(v+0.5)) \times 10^6,$$
$$G(0) = \omega_e/2.0 - \omega_e x_e/4.0 + \omega_e y_e/8.0,$$
$$G(v) = \omega_e(v+0.5) - \omega_e x_e(v+0.5)^2 + \omega_e y_e(v+0.5)^3,$$
$$G_0(v) = G(v) - G(0)$$

3.2.7. Extending the molecular line list

Several databases present updated line lists. Some of the most well known are described below:

Bertrand Plez's website[c] links to a directory of line lists in various formats. A constant update in line lists such as CH (Masseron et al. 2014) and NH (Fernando et al. 2018) carried out within TURBOSPECTRUM makes it extremely important to be able to implement these new data in other codes (and our own) by converting the formats from each other—see below and Section 3.3.1.

The Robert L. Kurúcz website[d] compiles several line lists converted to a standardised format (herein referred to as the 'Kurúcz format').

The High Resolution Transmission (HITRAN) brings molecular line lists, with description updated in Rothman et al. (2013).

As concerns complete line lists, the drawback is that they can reach millions of theoretical lines, with most of them being weak. The situation is similar to the millions of weak atomic lines (Kurúcz 1995). It is not our intent here to cover all these weak lines. This is accomplished, for example, by Tennyson &

[c] http://www.pages-perso-bertrand-plez.unaiv-montp2.fr.
[d] http://http://kurucz.harvard.edu/.

https://doi.org/10.1017/pasa.2018.33 Published online by Cambridge University Press

Yurchenko (2012), where laboratory and earlier calculations of molecular lines are completed by ab inition quantum mechanical treatment. Their line lists are presented in a standardised format using Einstein coefficients in the EXOMOL database.[e]

The webpage by Peter Bernath[f] contains a database on papers regarding a series of molecules.

The webpage by Jeremy Bailey[g] brings line lists, links to other databases, and software tools.

The *Virtual Atomic and Molecular Data Centre Consortium*—VAMDC[h] gives access to 36 inter-connected atomic and molecular databases (Dubernet et al. 2016).

Given all the different formats of the line lists available, line list conversion codes are valuable resources, as they allow for validations of synthesis codes and exchanges among research groups. We implemented a tool to convert molecular line lists from the Kurúcz formats (old and new) and also from the TURBOSPECTRUM/BSYN format, to the PFANT format, as described in Section 3.3.1. Other conversion paths are planned.

3.2.8. Output spectra

The code `pfant` generates three output files corresponding to the continuum, un-normalised flux, and normalised flux. As usual, the normalised flux is $\mathrm{flux}_{\mathrm{norm}}(\lambda) = \mathrm{flux}_{\text{un-normalised}}(\lambda)/\mathrm{flux}_{\mathrm{continuum}}(\lambda)$.

The code `nulbad` takes `pfant` output spectra, convolves it with a Gaussian profile (GP), and generates a file that, by default, contains the FWHM (full width at half maximum, given in Å) of the Gaussian profile in its name. This is a two-column text file with the wavelength (Å) and flux.

3.3. PYTHON interface and tools

With package `pyfant` (http://trevisanj.github.io/pyfant), one can write scripts that use PFANT spectral synthesis in the core of more complex tasks (e.g. automatic determination of stellar parameters) in the PYTHON language. The `pyfant` package application programming interface (API) includes resources to run PFANT spectral synthesis in series and in parallel, and to load, filter, transform, save, and visualise relevant data files.

In addition, `pyfant` contains a series of command-line and graphical tools (command-line and graphical interfaces) to perform various tasks, including a scraper of molecular constants from the NIST chemistry web book, an atomic lines converter from VALD3 to PFANT format, a molecular line list converter to the PFANT format, a tool to create grids of MARCS models, an editor for atomic lines, and an editor for molecular lines. A complete list of tools is obtained by running script `programs.py` in the computer terminal.

3.3.1. Conversion of molecular line lists

A systematic method to convert molecular line lists to the PFANT format was implemented. Conversion can be carried out with very little user interaction, provided that:

- Diatomic molecular constants are available in the NIST chemistry web book for the particular molecular systems of choice.[i]
- The input line list format contains sufficient information to determine the branch of each line.

In this section we discuss some particularities with the conversions of the Kurúcz and TURBOSPECTRUM line lists. For the Kurúcz format, the branch can be determined from the tabulated J', J'', $spin'$, and $spin''$ as follows:

- "P" if $J'' > J'$;
- "Q" if $J'' = J'$;
- "R" if $J'' < J'$.

And in more detail if it is 'P1', 'P2', 'P3', etc. is indicated by the spin of the lower state and upper states. If $spin'' = spin'$, the branch is '(P/Q/R)($spin$)', If $spin'' \neq spin$, the branch is '(P/Q/R)($spin'$)($spin''$)'.

TURBOSPECTRUM *line lists already contain the branch given as a string, for example, 'R23'.*

The branch is used to determine the specific formula from Kovács (1969) that will be used to calculate $\mathscr{S}_{J'J''}$. This choice of formula is a detailed procedure and depends on:

- the multiplicity of the transition (singlet, doublet, triplet);
- the sign and value of $\Delta\Lambda = \Lambda' - \Lambda''$;
- the sign of A; and
- the branch.

The Franck–Condon factors $q_{v'v''}$ (Equation 16) are computed with the code for transition probabilities of molecular transitions by Jarmain & McCallum (1970) (TRAPRB). The $q_{v'v''}$ factors are dependent on the system and the vibrational levels and have almost no dependence on rotational constants (Singh & de Almeida 1982).

The procedure described above *to convert molecular line lists* is coded as part of the `pyfant` API and is available as a graphical application named `convmol.py`. This application interfaces with the NIST chemistry web book to get the diatomic molecular constants A, B_e, α_e, β_e, ω_e, $\omega_e x_e$, and $\omega_e y_e$ (these can be later tuned if necessary), and interfaces with code TRAPRB to calculate $q_{v'v''}$.

3.4. Comparison with stellar spectra and code TURBOSPECTRUM

A validation of the code PFANT is presented here, with the comparison of the CN blue $B^2\Sigma - X^2\Sigma$ $(v' = 0, v'' = 0)$ bandhead (Figure 3), the CH $A^2\Delta - X^2\Pi$ (0,0) G-bandhead (Figure 4), and the NH $A^3\Pi - X^3\Sigma$ (0,0) bandhead (Figure 5) of the spectra resulting from the calculations with PFANT, TURBOSPECTRUM, and the observed solar spectrum (Kurúcz et al. 1984).

4. Summary

We present the description of calculation of diatomic molecular lines, given that this task is not straightforward. Molecular line intensities in the literature are given in either of the two formats: the Einstein A constant, related to the oscillator strength (see Section 2), or else the inclusion of all the ingredients that build together the oscillator strength.

[e] http://www.exomol.com/data/molecules
[f] http://bernath.uwaterloo.ca/molecularlists.php.
[g] http://newt.phys.unsw.edu.au/jbailey/vstar_mol.html.
[h] http://www.vamdc.edu.
[i] NIST is a convenient source because their data can be automatically retrieved using the tool `moldbed.py`. However, in some cases the NIST database does not contain the most recent data; so it is of interest to consult other databases, such as reported in Section 3.2.7.

https://doi.org/10.1017/pasa.2018.33 Published online by Cambridge University Press

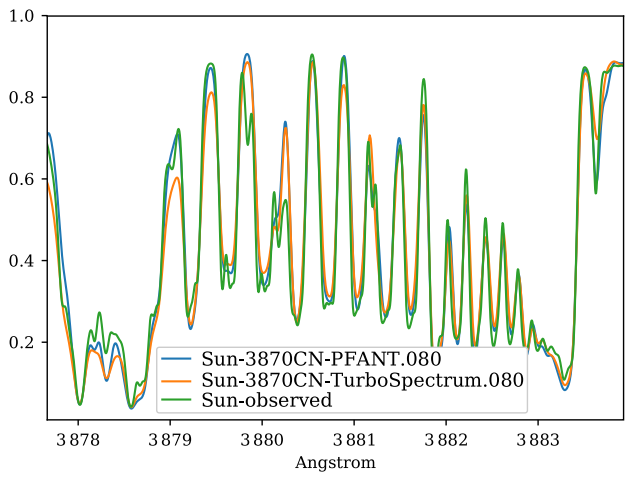

Figure 3. Synthetic and observed spectra of the the Sun, in the region of the CN $B^2\Sigma - X^2\Sigma$ (0,0) bandhead: observed spectrum (green); synthetic spectra with TURBOSPECTRUM (orange), and with PFANT (blue).

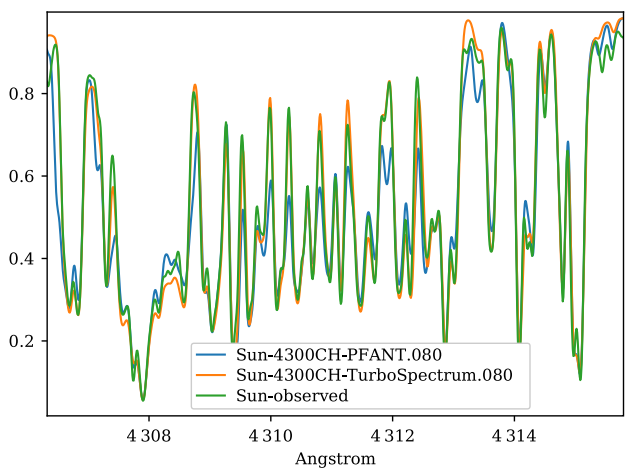

Figure 4. Synthetic and observed spectra of the the Sun, in the region of the CH $A^2\Delta - X^2\Pi$ (0,0) G-bandhead: observed spectrum (green); synthetic spectra with TURBOSPECTRUM (orange), and with PFANT (blue).

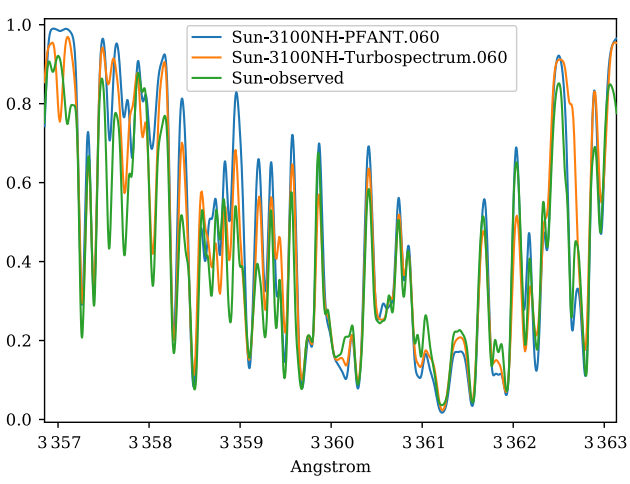

Figure 5. Synthetic and observed spectra of the the Sun, in the region of the NH $A^3\Pi - X^3\Sigma$ (0,0) bandhead: observed spectrum (green); synthetic spectra with TURBOSPECTRUM (orange), and with PFANT (blue).

We present a description of a new updated online version of the code for spectrum synthesis PFANT, together with many accessory tools and documentation. We describe the molecular line lists adopted, recalling that they need constant updating and implementation of new molecules. One example of an important update is the recent line list for NH (Fernando et al. 2018). The package includes codes for conversion of molecular line lists to the PFANT format, in particular so far from Kurúcz's and Plez's line lists. The atomic line list is also in constant improvement, both from the VALD3 database, as our own line list (available upon request).

Acknowledgements. We are grateful to the referee for constructive comments that helped improving the code and the paper. We thank J. Meléndez and R. Smiljanic for useful comments on a previous version of the manuscript. BB and AA acknowledge grants from CAPES—Finance code 001, CNPq and FAPESP. JT acknowledges the TT-5 FAPESP fellowships 2014/25987-5 and 2016/00777-3.

References

Abrams, M. C., Davis, S. P., Rao, M. L. P., Engleman, R., Jr., & Brault, J. W. 1994, ApJS, 93, 351
Alvarez, R., & Plez, B. 1998, A&A, 330, 1109
Anstee, S. D., O'Mara B. J. 1995, MNRAS, 276, 859
Asplund, M., Grevesse, N., Sauval, A. J., & Scott, P. 2009, ARA&A, 47, 481
Barbuy, B. 1982, PhD Thesis, Université de Paris VII
Barbuy, B., Perrin, M.-N., Katz, D., Coelho, P., Cayrel, R., Spite, M., & Van't Veer-Menneret, C. 2003, A&A, 404, 661
Barbuy, B., et al. 2011, A&A, 534, A60
Barbuy, B., et al. 2016, A&A, 591, A53
Barklem, P. S., Anstee, S. D., & O'Mara, B. J. 1998, PASA, 15, 336
Barklem, P. S., O'Mara, B. J. 1997, MNRAS, 290, 102
Barklem, P. S., Piskunov, N. E., & O'Mara, B. J. 2000, A&AS, 142, 467
Balfour, W. J., & Cartwright, H. M. 1976, A&AS, 26, 389
Bauschlicher, C. W., Langhoff, S. R., & Taylor, P. R. 1988, ApJ, 332, 531
Born, M., & Oppenheimer, R. 1927, Annalen der Physik, 389, 457
Brzozowski, J., Bunker, P., Elander, N., & Erman, P. 1976, ApJ, 207, 414
Castilho, B. V., Spite, F., Barbuy, B., Spite, M., de Medeiros, J. R., & Gregorio-Hetem, J. 1999, A&A, 345, 249
Cayrel, R., Perrin, M.-N., Barbuy, B., & Buser, R. 1991, A&A, 247, 108
Coelho, P., Barbuy, B., Meléndez, J., Schiavon, R. P., & Castilho, B. V. 2005, A&A, 443, 735
Davis, S. P., & Phillips, J. G. 1963, The Red System ($A^2\Pi$-$X^2\Sigma$) of the CN Molecule (Berkeley: University of California Press)
Dubernet, M.-L., Zwölf, C. M., Moreau, N., & Ba, Y. A. 2016, IAUFM, 29, 347
Duric, N., Erman, P., & Larsson, M. 1978, Phys. Scr., 18, 39
Edvardsson, B., Andersen, J., Gustafsson, B., Lambert, D. L., Nissen, P. E., & Tomkin, J. 1993, A&A, 275, 101
Einstein, A. 1917, PhyZ, 18, 121
Fernando, A. M., Bernath, P. F., Hodges, J. N., & Masseron, T. 2018, JQSRT, 217, 29
Gray, D. F. 2005, The Observation and Analysis of Stellar Atmospheres (3rd edn.; Cambridge: Cambridge University Press)
Grevesse, N., & Sauval, A. J. 1973, A&A, 27, 29
Grevesse, N., Noels, A., & Sauval, A. J. 1996, Standard Abundances, in *Cosmic Abundances*, eds. S. S. Holt, & G. Sonneborn, Astronomical Society of the Pacific Conference Series, 99, 117
Grevesse, N., Asplund, M., Scott, P., & Sauval, A. J. 2015, A&A, 573, A27
Goldman, A., Schoenfeld, W. G., Goorvitch, D., Chackerian, C., Dothe, H., Mélen, F., Abrams, M. C., & Selby, J. E. A. 1998, JQSRT, 59, 453
Goorvitch, D. 1994, ApJS, 95, 535
Gustafsson, B., Edvardsson, B., Eriksson, K., Jørgensen, U. G., Nordlund, Å., & Plez, B. 2008, A&A, 486, 951

Henneker, W. H., & Popkie, H. E. 1971, J. Chem. Phys., 54, 1763
Hönl, H., & London, F. 1925, ZA, 33, 803
Huber, K. P., & Herzberg, G. 1979, Molecular Spectra and Molecular Structure. IV. Constants of Diatomic Molecules (New York: Van Nostrand Reinhold Company), 716
Jarmain, W. R., & McCallum, J. C. 1970, TRAPRB, A Computer Programme for Molecular Transitions (Department of Physics, University of Western Ontario)
Jorgensen, U. G. 1994, A&A, 284, 179
Kirby, K., Saxon, R. P., & Liu, B. 1979, ApJ, 231, 637
Kovács, I. 1969, Rotational Structure in the Spectra of Diatomic Molecules (London: Adam Hilger Ltd.)
Kurúcz, R. L. 1970, SAO Special Report, 309.
Kurúcz, R. L. 1993a, Diatomic Molecular Data for Opacity Calculations. Kurucz CD-ROM No. 15. (Cambridge, Mass.: Smithsonian Astrophysical Observatory)
Kurúcz, R. L. 1995, Atomic Line Data (R. L. Kurucz and B. Bell) Kurucz CD-ROM No. 23. (Cambridge, Mass.: Smithsonian Astrophysical Observatory)
Kurúcz, R. L. 2017, Can. J. Phys., 95, 825
Kurúcz, R. L., Furenlid, I., Brault, J., & Testerman, L. 1984, National Solar Observatory Atlas (Sunspot, NM: National Solar Observatory)
Lambert, D. L. 1978, MNRAS, 182, 249
Luque, J., & Crosley, D. R. 1999, SRI Report No. MP 99-099
Masseron, T., et al. 2014, A&A, 571, A47
Meléndez, J., & Barbuy, B. 1999, ApJS, 124, 527
Meléndez, J., Barbuy, B., & Spite, F. 2001, ApJ, 556, 858
Pasquini, L., Ecuvillon, A., Bonifacio, P., & Wolff, B. 2008, A&A, 489, 315
Phillips, J. G., & Davis, S. P. 1968, The Swan System of the C_2 Molecule (Berkeley: University of California Press)
Phillips, J. G., Davis, S. P., Lindgren, B., & Balfour, W. J. 1987, ApJS, 65, 721
Piotto, G., Milone, A. P., & Bedin, L. R. 2015, AJ, 149, 91
Piskunov, N., & Valenti, J. A. 2017, A&A, 597, A16
Piskunov, N. E., Kupka, F., Ryabchikova, T. A., Weiss, W. W., & Jeffery, C. S. 1995, A&AS, 112, 525
Plez, B. 1998, A&A, 337, 495
Popovas, A. 2014, Master thesis, Niels Bohr Institute
Praderie, F. 1967, Ann. Ap., 30, 31
Pradhan, A. D., Partridge, H., & Bauschlicher, C. W., Jr. 1994, JChPh, 101, 3857
Rothman, L. S., et al. 2013, JQSRT, 130, 4
Ryabchikova, T., Piskunov, N., Kurucz, R. L., Stempels, H. C., Heiter, U., Pakhomov, Y., & Barklem, P. S. 2015, PhyS, 90, 054005
Schadee, A. 1964, BAN, 17, 311
Schadee, A. 1967, JQSRT, 7, 169
Schadee, A. 1971, A&A, 14, 401
Schadee A. 1975, A&A, 41, 203
Schadee, A. 1978, JQSRT, 19, 451
Schiavon, R. P., & Barbuy, B. 1999, ApJ, 510, 934
Schiavon, R. P., Barbuy, B., & Singh, P. D. 1997, ApJ, 484, 499
Schultz, R. H., & Armentrout, P. B. 1991, JChPh, 94, 2262
Scott, P., et al. 2015a, A&A, 573, A25
Scott, P., Asplund, M., Grevesse, N., Bergemann, M. & Sauval, A. J. 2015b, A&A, 573, A26
Singh, P. D., & de Almeida, A. 1982, JQSRT, 27, 471
Shetrone, M., et al. 2015, ApJS, 221, 24
Smiljanic, R., Gauderon, R., North, P., Barbuy, B., Charbonnel, C., Mowlavi, N. 2009, A&A, 502, 267
Smith, V. V., Terndrup, D. M., & Suntzeff, N. B. 2002, ApJ, 579, 832
Sneden, C. 1973, PhD thesis, U. of Texas at Austin
Spite, M. 1967, An. Ap. 30, 211
Spite, M., et al. 2005, A&A, 430, 655
Steffen, M., Prakapavičius, D., Caffau, E., Ludwig, H.-G., Bonifacio, P., Cayrel, R., Kučinskas, A., & Livingston, W. C. 2015, A&A, 583, A57
Tatum, J. B. 1967, ApJS, 14, 21
Tennyson, J., & Yurchenko, S. N. 2012, MNRAS, 425, 21
Tsuji, T. 1973, A&A, 23, 411
Trevisan, M., Barbuy, B., Eriksson, K., Gustafsson, B., Grenon, M., & Pompéia, L. 2011, A&A, 535, A42
Valenti, J. A., & Piskunov, N. 1996, A&AS, 118, 595
Whiting, E. E., & Nicholls, R. W. 1974, ApJS, 27, 1
Whiting, E. E., Schadee, A., Tatum, J. B., Hougen, J. T., & Nicholls, R. W. 1980, J. Mol. Spec., 80, 249

https://doi.org/10.1017/pasa.2018.33 Published online by Cambridge University Press